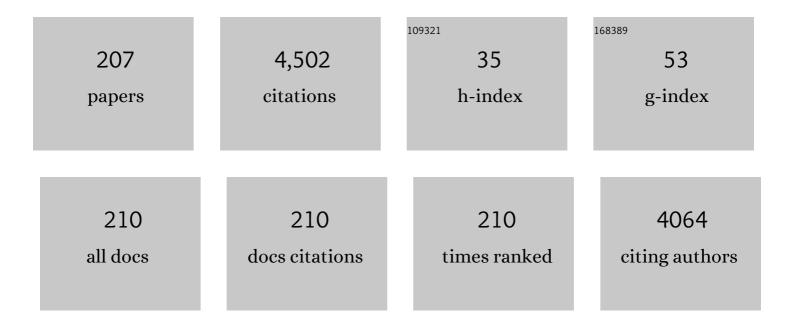
## Sergio Valeri

List of Publications by Year in descending order

Source: https://exaly.com/author-pdf/3820280/publications.pdf Version: 2024-02-01



SEDCIO VALEDI

#	Article	IF	CITATIONS
1	Tribological effects of surface texturing on nitriding steel for high-performance engine applications. Wear, 2008, 265, 1046-1051.	3.1	249
2	Evidence of Catalase Mimetic Activity in Ce <sup>3+</sup> /Ce <sup>4+</sup> Doped Bioactive Glasses. Journal of Physical Chemistry B, 2015, 119, 4009-4019.	2.6	119
3	Real-space determination of atomic structure and bond relaxation at theNiSi2-Si(111) interface. Physical Review Letters, 1985, 54, 827-830.	7.8	112
4	Nature of Ag Islands and Nanoparticles on the CeO <sub>2</sub> (111) Surface. Journal of Physical Chemistry C, 2012, 116, 1122-1132.	3.1	92
5	Oxide/Metal Interface Distance and Epitaxial Strain in theNiO/Ag(001)System. Physical Review Letters, 2003, 91, 046101.	7.8	87
6	Increasing nanohardness and reducing friction of nitride steel by laser surface texturing. Tribology International, 2009, 42, 699-705.	5.9	87
7	Morphology and optical properties of MgO thin films on Mo(001). Chemical Physics Letters, 2006, 430, 330-335.	2.6	83
8	AFM investigation of tribological properties of nano-patterned silicon surface. Wear, 2008, 265, 577-582.	3.1	80
9	Morphology, Stoichiometry, and Interface Structure of CeO <sub>2</sub> Ultrathin Films on Pt(111). Journal of Physical Chemistry C, 2011, 115, 10718-10726.	3.1	74
10	Auger electron emission by ion impact on solid surfaces. Surface Science Reports, 1993, 17, 85-150.	7.2	73
11	Structure and morphology of thin MgO films on Mo(001). Physical Review B, 2008, 78, .	3.2	65
12	Growth and structure of cobalt oxide on (001) bct cobalt film. Surface Science, 1999, 423, 346-356.	1.9	61
13	Comparing the deposition mechanisms in suspension plasma spray (SPS) and solution precursor plasma spray (SPPS) deposition of yttria-stabilised zirconia (YSZ). Journal of the European Ceramic Society, 2014, 34, 3925-3940.	5.7	61
14	The oxygen effect in the growth kinetics of platinum silicides. Journal of Applied Physics, 1981, 52, 6641-6646.	2.5	60
15	Nanoscale frictional behavior of graphene on SiO <sub>2</sub> and Ni(111) substrates. Nanotechnology, 2015, 26, 055703.	2.6	57
16	Interfacial interaction between cerium oxide and silicon surfaces. Surface Science, 2013, 607, 164-169.	1.9	56
17	Magnetic linear dichroism studies of in situ grown NiO thin films. Journal of Magnetism and Magnetic Materials, 2007, 310, 8-12.	2.3	52
18	Thickness-dependent strain in epitaxial MgO layers on Ag(). Surface Science, 2002, 507-510, 311-317.	1.9	49

#	Article	IF	CITATIONS
19	Experimental and theoretical study of the MgO/Ag() interface. Surface Science, 2002, 505, L209-L214.	1.9	48
20	Absence of oxide formation at the Fe/MgO(001) interface. Surface Science, 2005, 583, 191-198.	1.9	48
21	Correlation effects in valence-band spectra of nickel silicides. Physical Review B, 1984, 30, 5696-5703.	3.2	47
22	MODULATED ELECTRON EMISSION BY SCATTERING-INTERFERENCE OF PRIMARY ELECTRONS. Surface Review and Letters, 1997, 04, 141-160.	1.1	47
23	Interlayer water and swelling properties of monoionic montmorillonites. Journal of Colloid and Interface Science, 1981, 84, 301-309.	9.4	46
24	AFM nanoindentation: tip shape and tip radius of curvature effect on the hardness measurement. Journal of Physics Condensed Matter, 2008, 20, 474208.	1.8	46
25	Structural and morphological modifications of thermally reduced cerium oxide ultrathin epitaxial films on Pt(111). Physical Chemistry Chemical Physics, 2014, 16, 18848-18857.	2.8	46
26	Ion-beam-induced modification of Ni silicides investigated by Auger-electron spectroscopy. Physical Review B, 1983, 28, 4277-4283.	3.2	43
27	Iron Oxidation, Interfacial Expansion, and Buckling at theFe/NiO(001)Interface. Physical Review Letters, 2006, 96, 106106.	7.8	43
28	Nanostructured self-lubricating CrN-Ag films deposited by PVD arc discharge and magnetron sputtering. Vacuum, 2011, 85, 1108-1113.	3.5	43
29	Cerium-doped bioactive 45S5 glasses: spectroscopic, redox, bioactivity and biocatalytic properties. Journal of Materials Science, 2017, 52, 8845-8857.	3.7	43
30	Structure and morphology of ultrathin NiO layers on Ag(001). Thin Solid Films, 2003, 428, 195-200.	1.8	41
31	Structural study of thin MgO layers on Ag(001) prepared by either MBE or sputter deposition. Thin Solid Films, 2001, 400, 16-21.	1.8	39
32	Morphology evolution and magnetic properties improvement in FePt epitaxial films by in situ annealing after growth. Journal of Applied Physics, 2008, 103, 043912.	2.5	38
33	Polar and non-polar domain borders in MgO ultrathin films on Ag(001). Surface Science, 2005, 588, 160-166.	1.9	36
34	Competition between Polar and Nonpolar Growth of MgO Thin Films on Au(111). Journal of Physical Chemistry C, 2011, 115, 23043-23049.	3.1	36
35	Structure and stability of nickel/nickel oxide core–shell nanoparticles. Journal of Physics Condensed Matter, 2011, 23, 175003.	1.8	35
36	Deformation and Adhesion of Elastomer Poly(dimethylsiloxane) Colloidal AFM Probes. Langmuir, 2007, 23, 9293-9302.	3.5	33

#	Article	IF	CITATIONS
37	The analytical relations between particles and probe trajectories in atomic force microscope nanomanipulation. Nanotechnology, 2009, 20, 115706.	2.6	33
38	Growth of oxide-metal interfaces by atomic oxygen: Monolayer of NiO(001) on Ag(001). Physical Review B, 2009, 79, .	3.2	33
39	FIB assisted study of plasma sprayed splat–substrate interfaces: NiAl–stainless steel and alumina–NiAl combinations. Surface and Coatings Technology, 2010, 205, 363-371.	4.8	33
40	Frictional transition from superlubric islands to pinned monolayers. Nature Nanotechnology, 2015, 10, 714-718.	31.5	33
41	Ultrathin nickel oxide films grown on Ag(001): a study by XPS, LEIS and LEED intensity analysis. Surface Science, 2003, 531, 368-374.	1.9	32
42	Nano-structuration of CoO film by misfit dislocations. Surface Science, 2007, 601, 2651-2655.	1.9	32
43	Structure of Ultrathin CeO <sub>2</sub> Films on Pt(111) by Polarization-Dependent X-ray Absorption Fine Structure. Journal of Physical Chemistry C, 2013, 117, 1030-1036.	3.1	32
44	X-ray absorption near-edge structure and extended x-ray absorption fine-structure investigation of Pd silicides. Physical Review B, 1985, 32, 612-622.	3.2	31
45	Interplay between magnetocrystalline and configurational anisotropies in Fe(001) square nanostructures. Physical Review B, 2005, 72, .	3.2	31
46	Morphology and magnetic properties of size-selected Ni nanoparticle films. Journal of Applied Physics, 2010, 107, .	2.5	31
47	display="inline"> <mml:mrow><mml:mi mathvariant="normal">Mg</mml:mi><mml:mi mathvariant="normal"&gt;O<mml:mo>(</mml:mo><mml:mn>100</mml:mn><mml:mo>)</mml:mo><m mathvariant="normal"&gt;Ag<mml:mo>(</mml:mo><mml:mn>100</mml:mn><mml:mo>)</mml:mo><!--<br-->interfaces studied by<mml:math <="" td="" xmlns:mml="http://www.w3.org/1998/Math/MathML"><td>ml:mo&gt;â^• mml:mrow</td><td> &gt; </td></mml:math></m </mml:mi </mml:mrow>	ml:mo>â^• mml:mrow	 >
48	display="inline"> <mml:mrow></mml:mrow>		

#	Article	IF	CITATIONS
55	Self-organized growth of Ni nanoparticles on a cobalt-oxide thin film induced by a buried misfit dislocation network. Physical Review B, 2008, 77, .	3.2	28
56	Morphology-induced magnetic phase transitions in Fe deposits on MgO films investigated with XMCD and STM. Physical Review B, 2009, 79, .	3.2	28
57	Tribological characteristics of few-layer graphene over Ni grain and interface boundaries. Nanoscale, 2016, 8, 6646-6658.	5.6	28
58	Growth, structure and epitaxy of ultrathin NiO films on Ag(001). Thin Solid Films, 2001, 400, 139-143.	1.8	27
59	Growth and structure of Fe on MgO() studied by modulated electron emission. Surface Science, 2002, 498, 193-201.	1.9	27
60	Chemical reactions and interdiffusion at the Fe/NiO(001) interface. Surface Science, 2004, 572, L348-L354.	1.9	27
61	X-ray Photoemission Study of the Charge State of Au Nanoparticles on Thin MgO/Fe(001) Films. Journal of Physical Chemistry C, 2009, 113, 19957-19965.	3.1	27
62	Highly efficient plasmon-mediated electron injection into cerium oxide from embedded silver nanoparticles. Nanoscale, 2019, 11, 10282-10291.	5.6	27
63	Oxygen chemisorption and oxide formation on Ni silicide surfaces at room temperature. Surface Science, 1984, 145, 371-389.	1.9	26
64	Electrical and structural characterization of Nb-Si thin alloy film. Journal of Materials Research, 1986, 1, 327-336.	2.6	25
65	Development, operation and analysis of bialkali antimonide photocathodes for high-brightness photo-injectors. Nuclear Instruments and Methods in Physics Research, Section A: Accelerators, Spectrometers, Detectors and Associated Equipment, 1997, 385, 385-390.	1.6	25
66	Controlling single cluster dynamics at the nanoscale. Applied Physics Letters, 2009, 95, 143121.	3.3	25
67	Controlled growth of Ni/NiO core–shell nanoparticles: Structure, morphology and tuning of magnetic properties. Applied Surface Science, 2014, 306, 2-6.	6.1	25
68	Electrical, optical, and electronic properties of Al:ZnO films in a wide doping range. Journal of Applied Physics, 2015, 118, .	2.5	25
69	Atomic Scale Structure and Reduction of Cerium Oxide at the Interface with Platinum. Advanced Materials Interfaces, 2015, 2, 1500375.	3.7	25
70	AES study of room temperature oxygen interaction with near noble metal-silicon compound surfaces. Surface Science, 1985, 161, 1-11.	1.9	24
71	Surface-shift low-energy photoelectron diffraction: Clean and hydrogenated GaAs(110) surface-structure relaxation. Physical Review B, 1995, 51, 2399-2405.	3.2	24
72	K2Te photocathode growth: A photoemission study. Journal of Applied Physics, 2000, 87, 543-548.	2.5	24

#	Article	IF	CITATIONS
73	Magnetic couplings and exchange bias in Fe/NiO epitaxial layers. Physical Review B, 2010, 81, .	3.2	24
74	Steering the Growth of Metal Adâ€particles via Interface Interactions Between a MgO Thin Film and a Mo Support. Advanced Functional Materials, 2013, 23, 75-80.	14.9	24
75	Electronic properties of epitaxial cerium oxide films during controlled reduction and oxidation studied by resonant inelastic X-ray scattering. Physical Chemistry Chemical Physics, 2016, 18, 20511-20517.	2.8	24
76	Nanoindentation shape effect: experiments, simulations and modelling. Journal of Physics Condensed Matter, 2007, 19, 395002.	1.8	23
77	Tunability of exchange bias in Ni@NiO core-shell nanoparticles obtained by sequential layer deposition. Nanotechnology, 2015, 26, 405704.	2.6	22
78	Spin polarized photoemission from molecular beam epitaxy-grown be-doped GaAs. Zeitschrift Für Physik B Condensed Matter and Quanta, 1981, 44, 259-264.	1.9	21
79	Tribological Properties of High-Speed Uniform Femtosecond Laser Patterning on Stainless Steel. Lubricants, 2019, 7, 83.	2.9	21
80	NiO and MgO ultrathin films by polarization dependent XAS. Surface Science, 2004, 566-568, 84-88.	1.9	20
81	Growth and morphology of metal particles on MgO/Mo(001): A comparative STM and diffraction study. Physical Review B, 2011, 83, .	3.2	20
82	Valence photoemission study of temperature dependent reaction products in Ni-Si interfaces and thin films. Solid State Communications, 1982, 43, 199-202.	1.9	19
83	In-depth structural characterisation of the bct-hcp phase transition in Co epitaxial films. Europhysics Letters, 1999, 45, 501-507.	2.0	19
84	Structural and compositional stability of Co oxide grown on (001) bct Co. Applied Surface Science, 1999, 150, 13-18.	6.1	19
85	Hydrophobic effect of surface patterning on Si surface. Wear, 2010, 268, 488-492.	3.1	19
86	Anisotropy-graded magnetic media obtained by ion irradiation of L10 FePt. Acta Materialia, 2013, 61, 4840-4847.	7.9	19
87	Mesoporous bioactive glasses doped with cerium: Investigation over enzymatic-like mimetic activities and bioactivity. Ceramics International, 2019, 45, 20910-20920.	4.8	19
88	AES and EELS study of alkali-metal adsorption kinetics on either cleaved or sputtered GaAs and InP (110) surfaces. Surface Science, 1990, 238, 63-74.	1.9	18
89	Angular anisotropy of electron-excited secondary electron emission. Surface Science, 1994, 311, 422-432.	1.9	18
90	L2,3absorption edges inNi2Si. Physical Review B, 1986, 34, 2875-2877.	3.2	17

#	Article	IF	CITATIONS
91	Characterization of Cs2Te photoemissive film: formation, spectral responses and pollution. Nuclear Instruments and Methods in Physics Research, Section A: Accelerators, Spectrometers, Detectors and Associated Equipment, 1997, 393, 464-468.	1.6	17
92	Assembly and Fine Analysis of Ni/MgO Core/Shell Nanoparticles. Journal of Physical Chemistry C, 2011, 115, 14044-14049.	3.1	17
93	Influence of size, shape and core–shell interface on surface plasmon resonance in Ag and Ag@MgO nanoparticle films deposited on Si/SiO x. Beilstein Journal of Nanotechnology, 2015, 6, 404-413.	2.8	17
94	Influence of defect distribution on the reducibility of CeO <sub>2â^'<i>x</i></sub> nanoparticles. Nanotechnology, 2016, 27, 425705.	2.6	16
95	Structure of active cerium sites within bioactive glasses. Journal of the American Ceramic Society, 2017, 100, 5086-5095.	3.8	16
96	Graphene Confers Ultralow Friction on Nanogear Cogs. Small, 2021, 17, 2104487.	10.0	16
97	Morphology of H2O dosed monolayer MgO(001)/Ag(001). Surface Science, 2004, 566-568, 1071-1075.	1.9	15
98	Preparation and characterization of MgO stepped surfaces. Surface Science, 2007, 601, 2636-2640.	1.9	15
99	Local modifications of magnetism and structure in FePt (001) epitaxial thin films by focused ion beam: Two-dimensional perpendicular patterns. Journal of Applied Physics, 2008, 104, 053907.	2.5	15
100	Assembly and structure of Ni/NiO core–shell nanoparticles. Applied Surface Science, 2012, 260, 13-16.	6.1	15
101	Controlled co-deposition of FePt nanoparticles embedded in MgO: a detailed investigation of structure and electronic and magnetic properties. Nanotechnology, 2013, 24, 495703.	2.6	14
102	Chromium-Doped MgO Thin Films: Morphology, Electronic Structure, and Segregation Effects. Journal of Physical Chemistry C, 2015, 119, 25469-25475.	3.1	14
103	Dopant-Induced Diffusion Processes at Metal–Oxide Interfaces Studied for Iron- and Chromium-Doped MgO/Mo(001) Model Systems. Journal of Physical Chemistry C, 2016, 120, 13604-13609.	3.1	14
104	Cooling effect on the electron states of Si(III)î—,Pd and Si(III)î—,Pt interfaces. Solid State Communications, 1980, 35, 917-920.	1.9	13
105	Auger-electron emission induced byAr+impact on silicides. Physical Review B, 1988, 38, 13282-13290.	3.2	13
106	Role of Roughness Parameters on the Tribology of Randomly Nano-Textured Silicon Surface. Journal of Nanoscience and Nanotechnology, 2011, 11, 9244-9250.	0.9	13
107	NiO/Fe(001): Magnetic anisotropy, exchange bias, and interface structure. Journal of Applied Physics, 2013, 113, 234315.	2.5	13
108	Morphology, structural properties and reducibility of size-selected CeO <sub>2â^'</sub> <i><sub>x</sub></i> nanoparticle films. Beilstein Journal of Nanotechnology, 2015, 6, 60-67.	2.8	13

#	Article	IF	CITATIONS
109	Mechanical behaviour at ice-metal interfaces. Philosophical Magazine A: Physics of Condensed Matter, Structure, Defects and Mechanical Properties, 1978, 37, 17-26.	0.6	12
110	High energy (~ 107 eV) Si peak in Ar + excited auger emission from silicon and silicides. Surface Science, 1989, 220, 407-418.	1.9	12
111	Grain size reduction and magnetic properties improvement by in situ annealing of FePt epitaxial thin films. Journal of Magnetism and Magnetic Materials, 2007, 316, e158-e161.	2.3	12
112	Spontaneous Oxidation of Mg Atoms at Defect Sites in an MgO Surface. Journal of Physical Chemistry C, 2011, 115, 3684-3687.	3.1	12
113	Contraction, cation oxidation state and size effects in cerium oxide nanoparticles. Nanotechnology, 2017, 28, 495702.	2.6	12
114	Optical and electronic properties of silver nanoparticles embedded in cerium oxide. Journal of Chemical Physics, 2020, 152, 114704.	3.0	12
115	The Co/Si( 111 ) interface formation: a temperature dependent reaction. Surface Science, 2002, 511, 303-311.	1.9	11
116	Focused ion beam induced swelling in MgO(001). Surface Science, 2006, 600, 3718-3722.	1.9	11
117	Fe/NiO(100) and Fe/MgO(100) interfaces studied by X-ray absorption spectroscopy and non-linear Kerr effect. Superlattices and Microstructures, 2009, 46, 107-113.	3.1	11
118	Controlled AFM detachments and movement of nanoparticles: gold clusters on HOPG at different temperatures. Nanotechnology, 2012, 23, 245706.	2.6	11
119	Dynamics of the Interaction Between Ceria and Platinum During Redox Processes. Frontiers in Chemistry, 2019, 7, 57.	3.6	11
120	AES and EELS study of ErSi2 and its behaviour under ion bombardment and oxygen exposure. Solid State Communications, 1986, 60, 569-573.	1.9	10
121	Adsorption of monovalent metals on the GaAs(110) surface. Surface Science, 1987, 189-190, 226-231.	1.9	10
122	Focusing and defocusing in electron scattering along atomic chains. Physical Review B, 1994, 50, 14617-14620.	3.2	10
123	Fe epitaxial layers on Cu3Au(001): a structural study by primary-beam diffraction modulated electron emission. Surface Science, 2001, 471, 32-42.	1.9	10
124	Morphology and chemical activity at the Au/NiO interface. Surface Science, 2006, 600, 4251-4255.	1.9	10
125	Adhesion detachment and movement of gold nanoclusters induced by dynamic atomic force microscopy. Journal of Physics Condensed Matter, 2008, 20, 354011.	1.8	10
126	AFM-based tribological study of nanopatterned surfaces: the influence of contact area instabilities. Journal of Physics Condensed Matter, 2016, 28, 134008.	1.8	10

#	Article	IF	CITATIONS
127	Ion beam effects on the surface and near-surface composition of TaSi2. Nuclear Instruments & Methods in Physics Research B, 1991, 59-60, 98-101.	1.4	9
128	Diffraction effects in Auger quantitative analysis on Ill–V compounds. Applied Surface Science, 1993, 70-71, 20-23.	6.1	9
129	Auger electron spectroscopy for structural studies. Rivista Del Nuovo Cimento, 1993, 16, 1-73.	5.7	9
130	Element-specific, surface and subsurface structural analysis by scattering-interference of primary electrons. Journal of Electron Spectroscopy and Related Phenomena, 1995, 76, 723-728.	1.7	9
131	Structure and electronic properties of Fe nanostructures on MgO(001). Surface Science, 2007, 601, 3902-3906.	1.9	9
132	Interfacial magnetic structure in Fe/NiO(001). Physical Review B, 2011, 83, .	3.2	9
133	Cerium Oxide Epitaxial Nanostructures on Pt(111): Growth, Morphology and Structure. Topics in Catalysis, 2017, 60, 513-521.	2.8	9
134	Electron energy-loss spectroscopy of Ni2Si: Valence collective excitation and structural properties. Surface Science, 1986, 168, 204-211.	1.9	8
135	Correlation and autoionization effects in silicide Auger spectra. Thin Solid Films, 1986, 140, 89-94.	1.8	8
136	Electronic and vibrational properties of the K/GaAs system. Surface Science, 1989, 211-212, 659-665.	1.9	8
137	Metals on oxides: structure, morphology and interface chemistry. Journal of Physics Condensed Matter, 2007, 19, 225002.	1.8	8
138	Electrospun Fibers Containing Bioâ€Based Ricinoleic Acid: Effect of Amount and Distribution of Ricinoleic Acid Unit on Antibacterial Properties. Macromolecular Materials and Engineering, 2015, 300, 1085-1095.	3.6	8
139	Energy band associated with dangling bonds in silicon. Physical Review B, 1980, 22, 1926-1932.	3.2	7
140	Electron energy loss spectroscopic investigation of Cr-L2,3 core levels in Cr and chromium silicides. Solid State Communications, 1987, 61, 5-7.	1.9	7
141	Auger electron spectroscopy study of cleaved and sputter-etched In0.53Ga0.47As surfaces. Thin Solid Films, 1991, 197, 179-186.	1.8	7
142	Ion Beam-Stimulated Auger Electron Emission from Cr and Cr-Silicides. Physica Scripta, 1992, T41, 246-250.	2.5	7
143	Structural analysis of epitaxial Fe films on Ni(001). Applied Surface Science, 2000, 162-163, 198-207.	6.1	7
144	Imaging of the structure of ultra-thin cobalt silicide films by inelastically backscattered electrons. Applied Surface Science, 2001, 175-176, 83-89.	6.1	7

#	Article	IF	CITATIONS
145	Submicron-scale patterns on ferromagnetic–antiferromagnetic Fe/NiO layers by focused ion beam (FIB) milling. Nuclear Instruments & Methods in Physics Research B, 2005, 230, 512-517.	1.4	7
146	Initial stages of cobalt film growth on MgO(001) surface. Technical Physics Letters, 2005, 31, 494-497.	0.7	7
147	Depth-dependent magnetization reversal and spin structure of Fe/NiO exchange-coupled epitaxial bilayers. Applied Physics Letters, 2012, 101, 082412.	3.3	7
148	Auger electron spectroscopy study of the sputtering effect on platinum silicide surfaces. Thin Solid Films, 1985, 130, 315-326.	1.8	6
149	Importance of coulomb correlation in silicide spectra. Surface Science, 1986, 168, 164-170.	1.9	6
150	Ar+-induced silicon Auger spectra: a probe for the sputter-related collisional and emission processes. Nuclear Instruments & Methods in Physics Research B, 1991, 59-60, 37-40.	1.4	6
151	PLVV Auger lineshape modulation by incident beam diffraction in InP. Surface Science, 1993, 289, L617-L621.	1.9	6
152	Scattering interference of energetic electrons along atomic chains: The effect of the atomic environment. Physical Review B, 1995, 52, 14048-14057.	3.2	6
153	Substrate amorphization induced by the sputter deposition process: Geometrical aspects. Journal of Vacuum Science and Technology A: Vacuum, Surfaces and Films, 1995, 13, 394-399.	2.1	6
154	MODULATED ELECTRON EMISSION. Surface Review and Letters, 1997, 04, 937-945.	1.1	6
155	EPITAXY OF ULTRATHIN CoO FILMS STUDIED BY XPD AND GIXRD. Surface Review and Letters, 2002, 09, 937-941.	1.1	6
156	Thermally Sprayed Coatings as Interlayers for DLC-Based Thin Films. Journal of Thermal Spray Technology, 2009, 18, 231-242.	3.1	6
157	Depth-dependent magnetic characterization of Fe films on NiO(001). Nuclear Instruments & Methods in Physics Research B, 2010, 268, 361-364.	1.4	6
158	Ag Surface Diffusion and Out-of-Bulk Segregation in CrN-Ag Nano-Composite Coatings. Journal of Nanoscience and Nanotechnology, 2011, 11, 9260-9266.	0.9	6
159	Origin of Hydrophobicity in FIB-Nanostructured Si Surfaces. Langmuir, 2013, 29, 5286-5293.	3.5	6
160	Role of cerium oxide in bioactive glasses during catalytic dissociation of hydrogen peroxide. Physical Chemistry Chemical Physics, 2018, 20, 23507-23514.	2.8	6
161	Reducibility of Ag- and Cu-Modified Ultrathin Epitaxial Cerium Oxide Films. Journal of Physical Chemistry C, 2019, 123, 13702-13711.	3.1	6
162	Steering the magnetic properties of Ni/NiO/CoO core-shell nanoparticle films: The role of core-shell interface versus interparticle interactions. Physical Review Materials, 2017, 1, .	2.4	6

#	Article	IF	CITATIONS
163	GaAs and InP surface behaviour under ion bombardment, alkali deposition and oxygen exposure. Vacuum, 1990, 41, 643-646.	3.5	5
164	Growth and morphology of Te films on Mo. Thin Solid Films, 1999, 352, 114-118.	1.8	5
165	Pulsed laser ablation of glassy carbon targets for the coating of ion accelerator electrodes. Surface and Coatings Technology, 2001, 139, 87-92.	4.8	5
166	Magnetocrystalline and configurational anisotropies in Fe nanostructures. Journal of Magnetism and Magnetic Materials, 2005, 290-291, 183-186.	2.3	5
167	The Fe/NiO interface studied by polarization dependent X-ray absorption spectroscopy. Nuclear Instruments & Methods in Physics Research B, 2006, 246, 131-135.	1.4	5
168	Fe self-organization on stepped MgO surfaces. Superlattices and Microstructures, 2009, 46, 153-158.	3.1	5
169	Alkali metals adsorption kinetics on sputtered and cleaved GaAs(110) surfaces. Surface Science, 1991, 251-252, 995-999.	1.9	4
170	Interlaboratory tests of a composite reference sample to calibrate Auger electron spectrometers in the differential mode. Journal of Electron Spectroscopy and Related Phenomena, 1993, 61, 173-182.	1.7	4
171	Structural and electronic properties of thin Co films on Fe(001) and Fe(001)-p(1×1)O in the bct-to-hcp transition regime. Surface Science, 2000, 454-456, 671-675.	1.9	4
172	Structural characterisation of Fe layers on Co(112Ì,,0). Surface Science, 2000, 466, 30-40.	1.9	4
173	Ferromagnetic–antiferromagnetic Fe/NiO (100) interface studied by non-linear Kerr effect. Surface Science, 2007, 601, 4362-4365.	1.9	4
174	Magnetic anisotropy engineering in square magnetic elements. Journal of Magnetism and Magnetic Materials, 2007, 316, 106-109.	2.3	4
175	Effect of the indentation depth on the evaluation of mechanical properties of thin films. International Journal of Materials Research, 2008, 99, 847-851.	0.3	4
176	Orbital anisotropy in paramagnetic manganese oxide nanostripes. Physical Review B, 2013, 87, .	3.2	4
177	ZnO Nanostructure Formation on the Mo(001) Surface. Journal of Physical Chemistry C, 2015, 119, 13743-13749.	3.1	4
178	Ar+-beam-induced surface and subsurface modifications in Cr-Si compounds. Nuclear Instruments & Methods in Physics Research B, 1987, 19-20, 97-100.	1.4	3
179	Crystalline effects on Auger and photoelectron emission from clean and Cs-covered GaAs(110) surfaces. Applied Surface Science, 1992, 56-58, 205-210.	6.1	3
180	Auger lineshape modulation by scattering-interference of primary electrons. Journal of Electron Spectroscopy and Related Phenomena, 1995, 72, 299-303.	1.7	3

#	Article	IF	CITATIONS
181	Surface sensitivity of ion-induced Auger electron emission (IAE) spectroscopy. Surface Science, 1995, 331-333, 1256-1261.	1.9	3
182	Electron back-scattering contribution to the electron emission anisotropy by keV range electron beams. Journal of Electron Spectroscopy and Related Phenomena, 2001, 114-116, 477-482.	1.7	3
183	Structure and growth mode of thin Co films on Fe(001): comparison of purely thermal and ion-assisted deposition. Thin Solid Films, 2001, 397, 116-124.	1.8	3
184	Physical Synthesis and Study of Ag@CaF 2 Core@Shell Nanoparticles: Morphology and Tuning of Optical Properties. Physica Status Solidi (B): Basic Research, 2019, 256, 1800507.	1.5	3
185	Edge dislocation energy level in silicon. Physica Status Solidi A, 1978, 50, K123-K126.	1.7	2
186	Viscous layer at the ice surface. Solid State Communications, 1980, 35, 289-291.	1.9	2
187	Two hole spectra and valence states in chromium and chromium silicides. Journal of Electron Spectroscopy and Related Phenomena, 1987, 43, 121-130.	1.7	2
188	Ion bombardment influence on the Cr Auger autoionization structure. Solid State Communications, 1993, 86, 695-698.	1.9	2
189	Modulated electron emission for structural characterization of buried layers and interfaces. Progress in Surface Science, 1998, 59, 91-101.	8.3	2
190	Diamond-based composite layers as protective coatings for ion beam extraction systems. Journal of Vacuum Science and Technology A: Vacuum, Surfaces and Films, 2001, 19, 2920.	2.1	2
191	Breakdown of the bi-dimensional symmetry in bct Fe layers by epitaxy on Co(110) surface. Applied Surface Science, 2001, 175-176, 123-128.	6.1	2
192	Effects of structural nonplanarity on the magnetoresistance of Permalloy circular rings. Journal of Applied Physics, 2007, 101, 043901.	2.5	2
193	Secondary electron yield enhancement by MgO capping layers. Surface Science, 2010, 604, 181-185.	1.9	2
194	Core and valence excitations in Ni2Si. Thin Solid Films, 1986, 140, 99-104.	1.8	1
195	Local structure of Ni2Si. Journal of Electron Spectroscopy and Related Phenomena, 1987, 42, 287-292.	1.7	1
196	Effect of the incidence geometry on the ion induced Ni-silicides surface compositional modifications. Nuclear Instruments & Methods in Physics Research B, 1993, 80-81, 877-880.	1.4	1
197	Auger emission by impact of energetic atoms on Si monolayer(s). Surface Science, 1996, 365, 517-524.	1.9	1
198	Magnetism and morphology of Ni/Cu(1 0 0) and Ni–Fe–Ni/Cu(1 0 0) ultrathin films. Journal of Magnetism and Magnetic Materials, 2004, 272-276, E801-E802.	2.3	1

#	Article	IF	CITATIONS
199	Magnetoresistance of single Permalloy circular rings. Journal of Magnetism and Magnetic Materials, 2007, 316, e944-e947.	2.3	1
200	Growth and study of Ni nanoparticles films deposited on inert subtrates. Journal of Physics: Conference Series, 2008, 100, 072046.	0.4	1
201	Controlled manipulation of thiol-functionalised gold nanoparticles on Si (100) by dynamic force microscopy. Journal of Physics: Conference Series, 2008, 100, 052008.	0.4	1
202	Sliding onset of nanoclusters: a new AFM-based approach. Meccanica, 2011, 46, 597-607.	2.0	1
203	Tunable spin-wave frequency gap in anisotropy-graded FePt films obtained by ion irradiation. Physical Review B, 2016, 94, .	3.2	1
204	Particle-induced Auger emission from Si monolayers. Surface Science, 1996, 352-354, 719-723.	1.9	0
205	Evidence for interdot coupling in an array of micrometric Fe dots. Journal of Magnetism and Magnetic Materials, 2004, 272-276, E1373-E1375.	2.3	0
206	Structure of Reduced Cerium Oxide Ultrathin Films on Pt(111): Local Atomic Environment and Longâ€Range Order. Advanced Materials Interfaces, 2020, 7, 2000737.	3.7	0
207	Morphology and Friction Characterization of CVD Grown Graphene on Polycrystalline Nickel. Lecture Notes in Mechanical Engineering, 2014. , 195-204.	0.4	0